ELSEVIER

www.elsevier.nl/locate/jorganchem

Journal of Organometallic Chemistry 607 (2000) 137–145

Journal of Organometallic Chemistry

Reactions of heterometallic tungsten–iridium and tungsten–rhodium complexes containing C_4 chains

Michael I. Bruce [a,*], Benjamin G. Ellis [a], Brian W. Skelton [b], Allan H. White [b]

[a] *Department of Chemistry, University of Adelaide, Adelaide, South Australia 5005, Australia*
[b] *Department of Chemistry, University of Western Australia, Nedlands, Western Australia 6907, Australia*

Received 6 March 2000; accepted 8 May 2000

Dedicated with best wishes to Professor Martin Bennett, a valued friend and colleague, on the occasion of his retirement.

Abstract

Modified syntheses of $\{Cp(OC)_3W\}C{\equiv}CC{\equiv}C\{M(CO)(PPh_3)_2\}$ (M = Rh, Ir) from $W(C{\equiv}CC{\equiv}CH)(CO)_3Cp$ and $M(OTf)(CO)(PPh_3)_2$ are described. The Group 9 metal centre is the most electron-rich site, readily adding MeI or $C_2(CN)_4$. Reactions with iron carbonyls give successively $\{Cp(OC)_3W\}C{\equiv}CC_2\{Fe_2M(CO)_8(PPh_3)\}$ and $\{Cp(OC)_8Fe_2W\}C_2C_2\{Fe_2M(CO)_8(PPh_3)\}$, in which $Fe_2(CO)_6$ moieties add to a C≡C group and the adjacent metal centre. X-ray structures of $\{Cp(OC)_3W\}C{\equiv}CC{\equiv}C\{Rh(CO)[\eta\text{-}C_2(CN)_4](PPh_3)_2\}$, $\{Cp(OC)_3W\}C{\equiv}CC_2\{Fe_2Rh(CO)_8(PPh_3)\}$ and $\{Cp(OC)_8Fe_2W\}C_2C_2\{Fe_2Ir(CO)_8(PPh_3)\}$ have been determined.

Keywords: Tungsten; Rhodium; C_4 chains; Heterometallic

1. Introduction

The unusual electronic, magnetic and optical properties and reasonable non-linear optical properties that have been demonstrated for some metal complexes containing alkynyl, diynyl and higher poly-ynyl ligands has encouraged much of the contemporary interest in these species [1,2]. The potential of these compounds as molecular wires [3] has resulted in an increasing knowledge of their electronic structures, which may incorporate either alternating carbon–carbon single and triple bonds (**A**) and (**B**) or the cumulenic structure (**C**). The M–C single bonds or M≡C triple bonds in forms **A** and **B** may become important if the metal centre(s) is(are) redox-active.

$$\underset{(A)}{M\text{–}(C{\equiv}C)_n\text{–}M} \quad \underset{(B)}{M\text{–}(C{\equiv}C)_n\text{–}C{\equiv}M} \quad \underset{(C)}{M{=}(C{=}C)_n{=}M}$$

Several examples are known where electronic communication between the capping metal centres has been demonstrated, usually via cyclic voltammetry [4]. In the limit, they may approach one-dimensional carbon allotropes ('carbyne') [5].

We have been interested in examples of these complexes in which the carbon chain is capped by two different metal fragments and have recently described systems containing tungsten attached to metals of Groups 6–12 [6]. As far as we are aware, the only other heterometallic systems are those of Gladysz, who coupled his rhenium systems with palladium or rhodium in $\{Cp^*(Ph_3P)(NO)Re\}(C{\equiv}C)_n\{ML_n\}$ [$n = 1$, 2; $ML_n = PdCl(PEt_3)_2$, $Rh(CO)(PPh_3)_2$] [7]. Complexes containing the same metals with different ligands attached have been reported by Lapinte, who described the synthesis and redox properties of $\{Cp^*(dppe)Fe\}C{\equiv}CC{\equiv}C\{Fe(CO)_2Cp^*\}$ [4b]. In the present paper we describe modified syntheses of $\{Cp(OC)_3W\}C{\equiv}CC{\equiv}C\{M(CO)(PPh_3)_2\}$ (M = Rh, Ir) and some of their reactions, which illustrate the varying electronic properties of the $W\text{–}C_4\text{–}M$ chain.

* Corresponding author. Fax: +61-88-3035939; fax: +61-88-3034358.
E-mail address: michael.bruce@adelaide.edu.au (M.I. Bruce).

0022-328X/00/$ - see front matter
PII: S0022-328X(00)00309-0

2. Results and discussion

2.1. Syntheses of $\{Cp(OC)_3W\}C{\equiv}CC{\equiv}C\{M(CO)(PPh_3)_2\}$ (M = Ir, Rh)

The conditions under which our previous syntheses of $\{Cp(OC)_3W\}C{\equiv}CC{\equiv}C\{Ir(CO)(PPh_3)_2\}$ and its rhodium analogue were carried out resulted in the ready formation of the dioxygen adducts, of which the iridium derivative was crystallographically characterised, as a result of ready oxidative addition of O_2 to the Group 9 metal centres [6]. In the present work, we sought a more efficient coupling of $W(C{\equiv}CC{\equiv}CH)(CO)_3Cp$ to the iridium or rhodium centres and examined the reactions of $M(OTf)(CO)(PPh_3)_2$ (M = Rh, Ir) [8]. Accordingly, reactions of $W(C{\equiv}CC{\equiv}CH)(CO)_3Cp$ [9] with $M(OTf)(CO)(PPh_3)_2$, made in situ [10], in the presence of diethylamine, were performed in the strict absence of oxygen using standard Schlenk techniques to give the desired compounds $\{Cp(OC)_3W\}C{\equiv}CC{\equiv}C\{M(CO)(PPh_3)_2\}$ [M = Ir (**1**), Rh (**2**)] in high yield. Both complexes were isolated as bright yellow solids, which are sensitive to air, heat and light. All attempts to recrystallise these materials afforded mixtures with the dioxygen adducts described previously.

The infrared spectrum of a dioxygen-free sample of **1** shows two peaks in the carbonyl region at 2037 and 1952 cm^{-1} corresponding to the ν(CO) bands of the $W(CO)_3$ group. The Ir–ν(CO) peak in **1**, predicted to be at ca. 1955 cm^{-1} by comparison with that in $Ir(C{\equiv}CPh)(CO)(PPh_3)_2$ [11], is overlapped by the broad lower energy W–ν(CO) band at 1952 cm^{-1}. The corresponding bands in **2** are found at 2037 and 1952 cm^{-1}, but in this case the Rh–ν(CO) band is found at 1973 cm^{-1}. For **1**, the ν(CC) absorption occurs at 2115 cm^{-1}. The formation of the dioxygen adduct of **1** upon attempts at further purification was shown by the appearance of a new ν(CO) band in the IR spectrum at 2017 cm^{-1}, which was assigned to the ν(CO) absorption of the iridium(III) centre, together with the ν(OO) band at 832 cm^{-1}.

The ^{1}H-NMR spectra of **1** and **2** show singlet Cp resonances at δ 5.55 (Ir), 5.47 (Rh) and multiplets at δ 7.39–7.75 assigned to the Ph protons. The ^{13}C-NMR spectra contain resonances at δ 91.59 (Cp), between δ 128.1 and 134.9 (Ph) and three singlets at ca. δ 211, 231.6 (W–CO) and 240 (Ir/Rh–CO). Resonances of the carbon atoms of the chain in these and related complexes were not observed even with long delay and accumulation times.

Electrospray (ES) mass spectra of **1** show M^+ at m/z 1126, together with fragment ions at m/z 1098 ($[M - CO]^+$) and 745 ($[Ir(CO)(PPh)_2]^+$). For **2**, addition of NaOMe was necessary to enhance the spectrum [12] and resulted in the formation of an ion at m/z 1059 ($[M + Na]^+$), while in the negative ion spectrum $[M + OMe]^-$ was observed at m/z 1067.

2.2. Reactions of *1* and *2*

Complexes **1** and **2** contain four potential sites of electrophilic attack, namely the two metal atoms and the two C≡C triple bonds. To probe their reactivity, we have examined the reactions of **1** and **2** with iodomethane, tetracyanoethene (tcne) and iron carbonyl. The reaction with dioxygen suggested that the Group 9 metal is electron-rich, but other experiences with ethynylmetal complexes have shown that C_β is also a potential site for electrophilic attack [13]. Thus, while Vaska's complex readily adds iodomethane to give $IrMeClI(CO)(PPh_3)_2$ [14], the complex $Ru(C{\equiv}CPh)(PPh_3)_2Cp$ can be methylated to give the vinylidene $[Ru(=C{=}CMePh)(PPh_3)_2Cp]^+$ [15]. Reactions of $Ir(C{\equiv}CPh)(CO)(PPh_3)_2$ also occur at the iridium centre [11].

Similarly, addition of tetracyanoethene to Vaska's complex results in $IrCl(CO)\{\eta\text{-}C_2(CN)_4\}(PPh_3)_2$ [16], in which the iridium centre is formally oxidised to Ir(III), with ν(CO) at 2060 cm^{-1}. In contrast, tcne reacts with $Ru(C{\equiv}CPh)(PPh_3)_2Cp$ to give the butadienyl complex $Ru\{C[=C(CN)_2]{=}CPhC(CN)_2\}(PPh_3)_2Cp$, which readily loses PPh_3 to give $Ru\{\eta^3\text{-}C(CN)_2CPhC{=}C(CN)_2\}(PPh_3)Cp$, the initial reaction occurring by addition of the electron-deficient olefin to the σ-bonded alkynyl group [17]. With $Rh(C{\equiv}CPh)(CO)(PPh_3)_2$, addition occurs to the metal centre [18], while with $W(C{\equiv}CC{\equiv}CH)(CO)_3Cp$, addition occurs at the C≡C triple bond further from the tungsten atom [9].

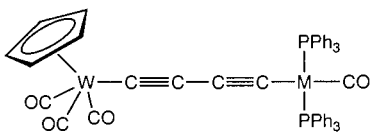

M = Ir (**1**), Rh (**2**)

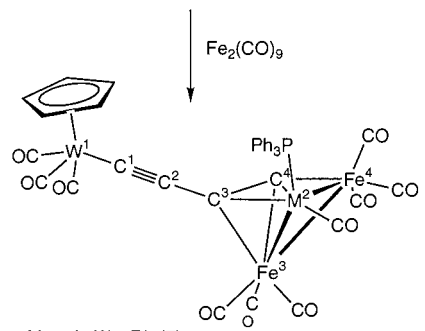

M = Ir (**6**), Rh (**7**)

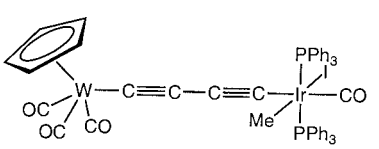

(**3**)

2.3. Reaction of **1** with iodomethane

The reaction between **1** and MeI was carried out in thf and afforded $\{Cp(OC)_3W\}C{\equiv}CC{\equiv}C\{IrMeI(CO)(PPh_3)_2\}$ (**3**) in 76% yield. This complex was identified spectroscopically and from elemental analysis. In particular, addition at Ir confirmed by the shift in the Ir ν(CO) band to 2047 cm^{-1}, indicating a change in the formal oxidation state at the iridium centre from +1 to +3. The ^{1}H-NMR spectrum of **3** contains a triplet resonance at δ 0.68 (Me) and a singlet at 5.54 (Cp) in addition to the Ph multiplet between δ 7.32 and 8.03. The ^{13}C-NMR spectrum contained resonances at δ 1.11 (Me), 91.64 (Cp) and a multiplet between δ 127.63 and 131.72 (Ph). Two W–CO resonances were at δ 230.76 and 210.89 ppm, while the Ir–CO resonance at δ 169.15 also confirms the presence of the Ir(III) centre, removal of electron density from the metal causing an upfield shift of ca. 70 ppm. The stereochemistry of the product however could not be deduced unequivocally. In this regard, we note that it was recently reported that addition of H_2 or HC≡CPh to $Ir(C{\equiv}CPh)(CO)(PPh_3)_2$ affords the *cis*,*trans* isomer of $IrH(X)(C{\equiv}CPh)(CO)(PPh_3)_2$ (X = H or C≡CPh) (corresponding to **3b**) by rapid intramolecular rearrangement of the first-formed *cis*,*cis* isomer (corresponding to **3c**) [19].

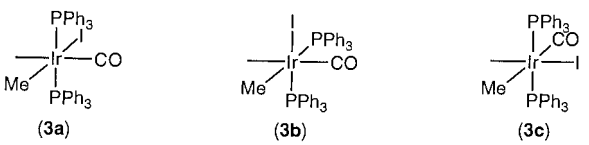

2.4. Reactions with tetracyanoethene (tcne)

The reactions of **1** or **2** with one equivalent of tcne in THF gave $\{Cp(OC)_3W\}C{\equiv}CC{\equiv}C\{M(CO)[\eta\text{-}C_2(CN)_4](PPh_3)_2\}$ [M = Ir (**4**), Rh (**5**)] as yellow and orange crystalline solids, respectively. Attempts to add a second tcne molecule to **4** proved unsuccessful. The formulas of **4** and **5** were established by elemental microanalysis and spectroscopically and confirmed by a single-crystal X-ray structure determination of **5**. The IR spectrum of **4** contained ν(CN) at 2227 cm^{-1} and three ν(CO) bands at 2058, 2039 and 1952 cm^{-1}. Of these, the bands at 2039 and 1952 cm^{-1} can be assigned to the $W(CO)_3Cp$ group, while that at 2058 cm^{-1} arises from the Ir–CO ligand, reflecting the presence of the formal Ir(III) centre. For **5**, these absorptions were found at 2224 [ν(CN)] 2078, 2039 and 1953 cm^{-1} [ν(CO)]; additionally, the ν(CC) absorption was found at 2142 cm^{-1}.

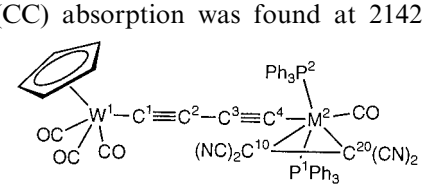

M = Ir (**4**), Rh (**5**)

The ^{1}H-NMR spectra of **4** and **5** contain singlets at δ ca. 5.5 (Cp) and multiplets between δ 7.26 and 7.52 (Ph), while the ^{13}C-NMR spectra have multiplets between δ 128.32 and 134.26 (Ph), with three singlets at δ ca. 230.7, 211.1 (W–CO) and 170.0 (Ir–CO; the Rh–CO resonance was not observed). The low-field signal found for the latter again confirms the presence of an oxidised iridium centre. Singlet CN resonances were found at δ 112.6 and 116.9.

2.5. Molecular structure of $\{Cp(OC)_3W\}C{\equiv}CC{\equiv}C\{Rh(CO)[\eta\text{-}C_2(CN)_4](PPh_3)_2\}$ (**5**)

Fig. 1 is a representation of a molecule of $\{Cp(OC)_3W\}C{\equiv}CC{\equiv}C\{Rh(CO)[\eta\text{-}C_2(CN)_4](PPh_3)_2\}$ (**5**) and significant bond parameters are collected in Table 1. As can be seen, the acetylenic hydrogen in $W(C{\equiv}CC{\equiv}CH)(CO)_3Cp$ has been replaced by a rhodium [Rh–C(4) 2.00(1) Å], to which are attached the CO group [Rh–CO 1.86(1) Å], two PPh_3 ligands [Rh–P 2.380, 2.393(4) Å], and the tetracyanoethene ligand. The latter is bonded to Rh via C(10) and C(20) in the usual side-on η^2 mode [Rh–C(10, 20) 2.15, 2.16(1) Å]. The geometry is very similar to that of the same ligand in $Rh(C{\equiv}CPh)\{\eta\text{-}C_2(CN)_4\}(NCMe)(PPh_3)_2$ [18] or $IrBr(CO)(AsPh_3)_2\{\eta\text{-}C_2(CN)_4\}$ [20]. The coordination geometry about rhodium is trigonal bipyramidal (considering the tcne ligand to occupy one site), the two PPh_3 ligands occupying equatorial sites [P(1)–Rh–P(2) 110.2(1)°, cf. 107.43(6)° in the Ir complex]. The C(10)–C(20) bond [1.49(2) Å, cf. 1.447(23) Å in the Ir complex] is ca. 0.15 Å longer than that found in free tcne [1.344(3) Å] [21]. Distortion of the tcne ligand from planarity also occurred as expected, with the four CN substituents bent away from the metal, as found in other examples of complexes containing this ligand [18,20,22].

Comparison of the tungsten moiety also reveals little difference from related compounds. The C_4 bridge is non-linear, with angles at C(1,2,3,4) ranging between 170 and 178(1)°. The M–C bond lengths are 2.10(1) (W) and 2.00(1) Å (Rh) [cf. 2.148(4) in $W(C{\equiv}CC{\equiv}CH)(CO)_3Cp$ [23], 1.94(2) Å in $Rh(C{\equiv}CPh)\{\eta\text{-}C_2(CN)_4\}(NCMe)(PPh_3)_2$] [18].

2.6. Reactions with $Fe_2(CO)_9$

Iron carbonyls readily form mixed-metal cluster complexes, such as $Fe_2W(\mu_3\text{-}C_2R)(CO)_8Cp$ (R = Ph [24], tol [25]) with $W(C{\equiv}CR)(CO)_3Cp$, and $Fe_2M(\mu_3\text{-}C_2R)(CO)_8(PPh_3)$ (M = Ir, Rh) in reactions with Group 9 alkynyls [26]. The reactions of **1** and **2** with $Fe_2(CO)_9$ were carried out to determine the site(s) of addition to these mixed-metal diyndiyl systems. Two major products were isolated from reactions of **1** or **2** with an excess of

$Fe_2(CO)_9$, which could be separated by preparative TLC. They were characterised by elemental analyses and spectroscopic methods as $\{Cp(OC)_3W\}C{\equiv}CC_2\{Fe_2M(CO)_8(PPh_3)\}$ [M = Ir (**6**), Rh (**7**)] and $\{Cp(OC)_8Fe_2W\}C_2C_2\{Fe_2M(CO)_8(PPh_3)_3\}$ [M = Ir (**8**), Rh (**9**)], the structures being confirmed by single-crystal structural determinations for **7** and **8**.

For **6** and **7**, the IR spectra contained similar complex ν(CO) patterns between 1950 and 2068 cm^{-1}. The ^{1}H-NMR spectra of the two complexes contained singlet resonances at δ 5.62 and 5.49 (Cp) and multiplets between δ 7.26 and 7.50 (Ph). The relative intensities of the latter confirmed that one PPh_3 ligand has been lost from the Group 9 metal centre, probably in combination with an $Fe(CO)_4$ fragment. In the ^{13}C-NMR spectra, singlets at δ ca. 88.4 or 91.72 (Cp) and phenyl multiplets between δ 128.8 and 134.2 were found. At low field, only signals at ca. δ 218.5 (W–CO) and 212.0 (Fe–CO) were observed, with a singlet at δ 167.7 being assigned to the Rh–CO resonance, the Ir–CO signal not being found. In the ES mass spectra of solutions of **6** and **7** containing NaOMe, the base peak is $[M + OMe]^-$, at m/z 1202 and 1084, respectively.

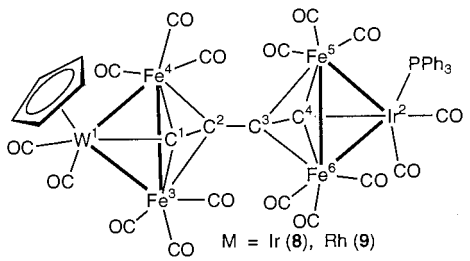

The second product isolated from each reaction has the formula $\{Cp(OC)_8Fe_2W\}C_2C_2\{Fe_2M(CO)_8(PPh_3)\}$ [M = Ir (**8**), Rh (**9**)]. The rhodium complex was obtained in very low yield, possibly because of the thermal instability of **2**. As for **6** and **7**, the IR ν(CO) spectra of **8** and **9** are complex. The ^{1}H-NMR spectrum of **8** contains a singlet resonance for the Cp protons at δ 5.63, with a Ph multiplet at δ ca. 7.34–7.70, the latter signal arising from only one PPh_3 ligand. The ^{13}C-NMR spectrum of **8** contains a Cp singlet resonance at δ 91.94 and a Ph multiplet at δ ca. 128.57–133.74. Peaks at δ 212.39 and 210.54 arise from Fe–CO ligands on the two different iron clusters. The Ir–CO ligands give a singlet at δ 174.80 and the W–CO groups are found at δ 227.94. There does not appear to be any intermetal exchange for these CO ligands. ES mass spectra (negative ion mode with NaOMe) of **8** have as the base peak $[M + OMe]^+$ at m/z 1454. An MS/MS experiment showed fragmentation to $[(M + OMe) - nCO]^-$ ($n = 4$, 8 and 11). In the ES mass spectrum of **9**, the highest ion at m/z 1335 corresponds to $[M + H]^+$; an MS–MS experiment on this ion showed fragmentation by loss of CO, PPh_3 and $Fe_2(CO)_4$ groups.

Addition of $Fe_2(CO)_9$ to both **6** and **7** resulted in their conversion to the di-cluster complexes **8** and **9**, respectively, suggesting that the mono-cluster compounds are in fact intermediates in the formation of the di-cluster complexes **8** and **9**.

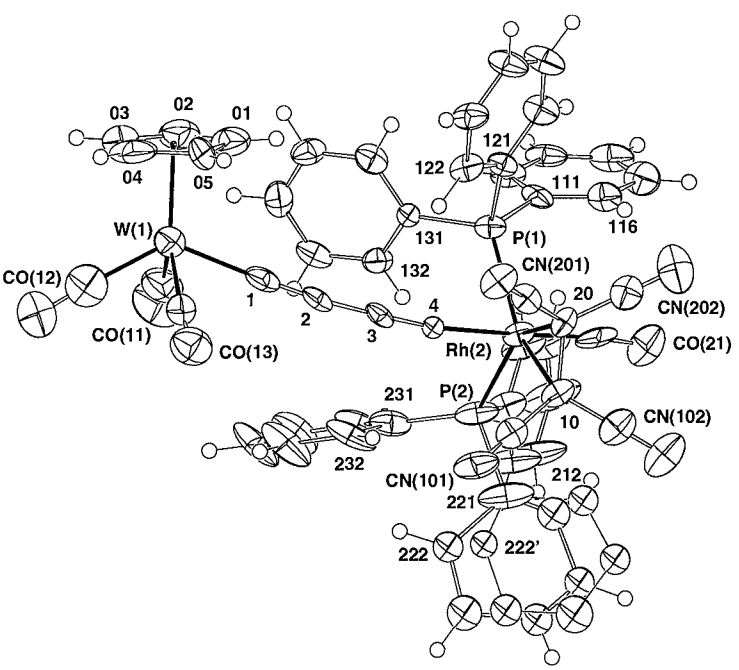

Fig. 1. Plot of a molecule of $\{Cp(OC)_3W\}C{\equiv}CC{\equiv}C\{Rh(CO)[\eta\text{-}C_2(CN)_4](PPh_3)_2\}$ (**5**), showing atom numbering scheme. In this and subsequent figures, non-hydrogen atoms are shown as 20% thermal ellipsoids; hydrogen atoms have arbitrary radii of 0.1 Å.

Table 1
Selected bond distances (Å) and bond angles (°) in complexes **5**, **7** and **8**

Bond	5	7	8
Bond distances [a]			
W–C(Cp)	2.30–2.39(1)	2.304–2.376(4)	2.296–2.330(10)
(av.)	2.33	2.34	2.31
W–CO	1.94–2.05(2)	2.002–2.012(4)	1.982, 2.01(1)
(av.)	1.99	2.006	1.996
W–C(1)	2.10(1)	2.125(3)	1.978(7)
Fe–CO		1.786–1.816(4)	
(av.)		1.799	
Fe(3)–Fe(4)		2.6369(6)	2.530(2)
Fe(5)–Fe(6)			2.495(2)
Fe(3)–M		2.5727(6) (Rh)	2.875(1) (W)
Fe(4)–M		2.7119(5) (Rh)	2.8456(9) (W)
Fe(5)–M			2.726(1) (Ir)
Fe(6)–M			2.6787(9) (Ir)
M–P(1)	2.380(3) (Rh)	2.4152(9) (Rh)	2.340(2) (Ir)
M–P(2)	2.393(4) (Rh)		
M–C(2n)	1.86(1) (Rh)	1.912, 1.934(2) (Rh)	1.917, 1.907(9) (Ir)
M–C(3)		2.223(2) (Rh)	
M–C(4)	2.00(1) (Rh)	2.160(3) (Rh)	1.929(7) (Ir)
Fe(3)–C(1)			2.028(8)
Fe(3)–C(2)			2.111(8)
Fe(3)–C(3)		2.105(3)	
Fe(3)–C(4)		2.008(3)	
Fe(4)–C(I)			2.038(6)
Fe(4)–C(2)			2.036(7)
Fe(4)–C(4)		1.812(2)	
Fe(5)–C(3)			2.113(8)
Fe(5)–C(4)			2.018(7)
Fe(6)–C(3)			2.085(7)
Fe(6)–C(4)			2.076(6)
C(1)–C(2)	1.23(2)	1.218(3)	1.313(8)
C(2)–C(3)	1.38(2)	1.394(3)	1.42(1)
C(3)–C(4)	1.20(2)	1.323(3)	1.309(8)
Bond angles [b]			
c(1)–W–C(11)	74.6(6)		121.8(3)
C(1)–W–C(12)	131.1(6)	126.2(1)	96.0(3)
C(1)–W–C(13)	77.2(6)	73.8(1)	
P(1)–Rh–P(2)	110.2(1)		
C(4)–Rh–C(21)	176.3(5)		
P(1)–Rh–C(21)	95.7(4)		
P(2)–Rh–C(21)	87.8(4)		
P(1)–Rh–C(4)	81.4(3)		
P(2)–Rh–C(4)	91.2(3)		
Fe(3)–M–P		148.55(2) (Rh)	
Fe(5)–M–P			108.38(5) (Ir)
W–C(1)–C(2)	178(1)	177.4(3)	158.9(5)
C(1)–C(2)–C(3)	173(1)	175.2(3)	146.1(6)
C(2)–C(3)–C(4)	176(1)	150.1(2)	149.1(6)
C(3)–C(4)–M	170(1) (Rh)	156.4(2) [Fe(4)]	153.2(5) (Ir)

[a] Other distances. For **5**: M–C(10), 2.15(1); M–C(20), 2.16(1); C(10)–C(20), 1.49(2); P(1)–Rh–C(10/20), 125.5(3); P(2)–Rh–C(10/20), 123.8(3).

[b] Other angles: Rh(2)–C(10)–C(101,102), 115.9(8), 116.7(9); Rh(2)–C(20)–C(201,202), 120.0(8), 111.5(9)°. C(20)–C(10)–C(101,102) are 120(1), 116(1); with C(101)–C(10)–C(102), 112(1) (Σ 348°); C(10)–C(20)–C(201,202) are 117(1), 118(1); with C(201)–C(20)–C(202), 114(1)° (Σ 348°).

*2.7. Molecular structures of $\{Cp(OC)_3W\}C{\equiv}CC_2\{Fe_2Rh(CO)_8(PPh_3)\}$ (**7**) and $\{Cp(OC)_8Fe_2W\}C_2C_2\{Fe_2Ir(CO)_8(PPh_3)\}$ (**8**)*

Figs. 2 and 3 contain plots of molecules of **7** and **8**, respectively, with important bond parameters being summarised in Table 1. Direct comparisons can be made with the previously described cluster complexes $Fe_2W(\mu_3\text{-}C_2R)(CO)_8Cp$ [24,25] and $Fe_2Ir(\mu_3\text{-}C_2Ph)(CO)_8(PPh_3)$ [26]. In **7**, addition of an $Fe_2(CO)_6$ unit to the rhodium centre formed an Fe_2Rh cluster, which carries eight CO groups and the remaining PPh_3 ligand. Two carbons of the C_4 chain interact with this cluster in the usual $2\sigma,\pi$ mode, with C(4) being σ-bonded to Fe rather than Rh, as in precursor **2**. Such rearrangement is not unexpected, being the result of the ready mobility of alkynyl groups (although not found here) around

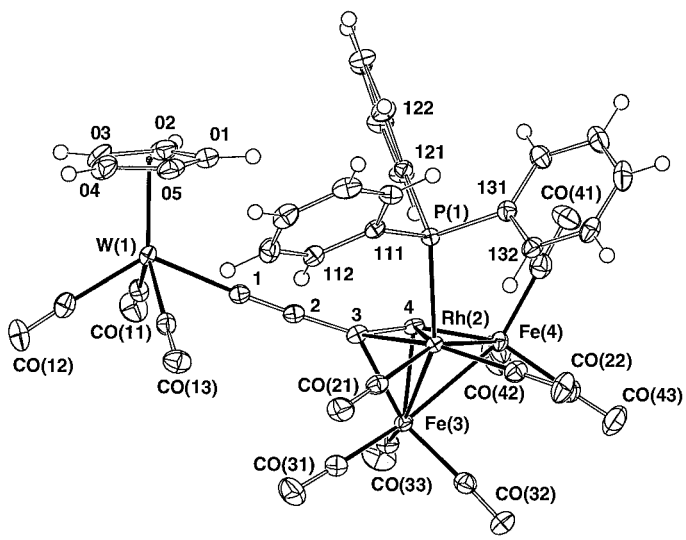

Fig. 2. Plot of a molecule of $\{Cp(OC)_3W\}C{\equiv}CC_2\{Fe_2Rh(CO)_8(PPh_3)\}$ (**7**), showing atom numbering scheme.

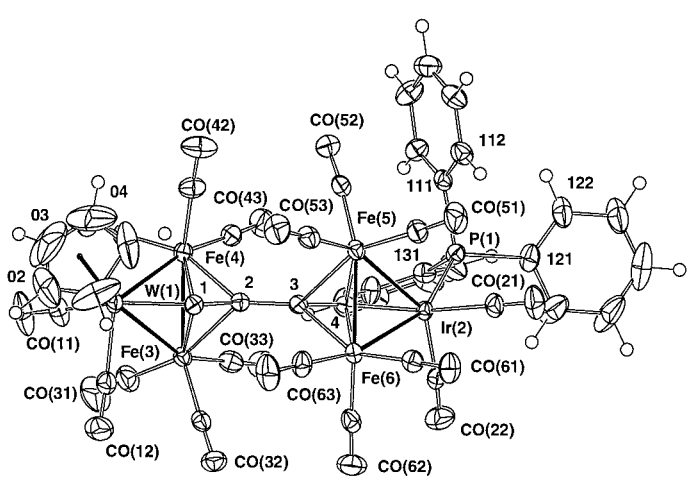

Fig. 3. Plot of a molecule of $\{Cp(OC)_8Fe_2W\}C_2C_2\{Fe_2Ir(CO)_8(PPh_3)\}$ (**8**), showing atom numbering scheme.

clusters [27]. A homometallic example is found in $Fe_3(\mu_3\text{-}C_2Ph)(\mu\text{-}CO)(CO)_7Cp$, obtained from $Fe(C{\equiv}CPh)(CO)_2Cp$ and $Fe_2(CO)_9$, in which the C_2Ph and Cp groups are attached to different iron atoms [28]. The Fe–Fe bond in **7** [2.6369(6) Å] is similar to that found in $Fe_2W\{\mu_3\text{-}C(tol)\}\{\mu\text{-}C_2(SiMe_3)_2(\mu\text{-}CO)(CO)_6Cp$ [29], while the two Fe–Rh bonds differ significantly [Fe(1,2)–Rh 2.5727(6), 2.7119(5) Å], reflecting the different electron density at each iron, resulting from the σ or π coordination of the C_2 unit. For comparison, the Fe–Rh distances in $Fe_2Rh(\mu\text{-}H)(\mu_3\text{-}COMe)(CO)_7Cp$ are 2.634 and 2.652(1) Å [30]. The alkynyl substituent in **7** is the $-C{\equiv}CW(CO)_3Cp$ group and is bent away from the cluster [C(2)–C(3)–C(4) 150.1(2)°]; the corresponding angle at C(4) is 156.4(2)°. The $W(CO)_3Cp$ group is similar to that in **5**, with angles along the chain at C(1) and C(2) being 177.4(3) and 175.2(3)°, respectively.

In complex **8**, addition of the second $Fe_2(CO)_6$ unit occurred at tungsten to give an Fe_2W cluster with loss of a CO ligand. Metal–metal separations are 2.495(2), 2.530(2) (Fe–Fe), 2.6787(9), 2.726(1) (Fe–Ir), 2.8456(9) and 2.875(1) Å (Fe–W). The differences between the various values can be ascribed to the differences in local coordination, e.g. the two Fe–Fe distances are found in different clusters, the two Fe–Ir distances are *trans* to CO and PPh_3, while the two Fe–W bonds are *trans* to CO and Cp, respectively. The Fe–W distances are longer than those found in $Fe_2W\{\mu_3(tol)\}\{\mu\text{-}C_2(SiMe_3)_2\}(\mu\text{-}CO)(CO)_6Cp$ [29] and $Fe_2W\{\mu_3\text{-}C(tol)\}(\mu\text{-}CO)(CO)_8Cp$ [2.756, 2.805(2) Å] [30]. The C_4 chain is now complexed to both cluster cores, the two C_2 units both being attached in the 2σ,π mode with the σ bonds between C(1) and W [1.978(7) Å] and, in contrast with **7**, between C(4) and Ir [1.929(7) Å]. The C_4 chains are no longer linear, with angles at C(1,2,3,4) ranging between 146.1(6) and 158.9(5)°, comparable with those found in other examples of C_2FeM (M = Ir, W) clusters mentioned above. It is notable that the C_2Fe_2Ir and C_2Fe_2W clusters are joined only by the C(2)–C(3) bond [1.42(1) Å] as has been found before in the anion $[\{Fe_3(CO)_9\}(\mu\text{-}C_2C_2)]^{2-}$, in which the separation is 1.42(1) [31]. Similarly, the angles at the central carbons are 146.1 and 149.1(6)° in **8**, which may be compared with the value of 148.0(6)° in the cluster dianion. In both examples, the C_4 chains adopt a transoid geometry.

3. Conclusions

The complexes $\{Cp(OC)_3W\}C{\equiv}CC{\equiv}C\{M(CO)(PPh_3)_2\}$ where M = Rh or Ir have been prepared successfully by a new synthetic method involving reactions of triflate derivatives with $W(C{\equiv}CC{\equiv}CH)(CO)_3Cp$. Although these complexes were light and air sensitive, it was found that they can be stored in a cold and dark environment with little decomposition occurring over several months. The reactions of these complexes revealed that the Group 9 metal was the most electron-rich site in the molecule. Thus, oxidative addition reactions with MeI and tcne have given complexes in which the Group 9 metal is formally oxidised. Reactions of **1** and **2** with $Fe_2(CO)_9$ result in addition of $Fe_2(CO)_6$ moieties firstly to the C≡C triple bond adjacent to the Group 9 metal, and then to the C≡C triple bond adjacent to the tungsten. From these reactions, mixed-metal clusters incorporating either two or four carbons of the C_4 chain have been obtained, but it has not been possible to attach all four carbons to a single polymetallic cluster.

4. Experimental

4.1. General reaction conditions

All reactions were carried out under dry, high purity nitrogen using standard Schlenk techniques. Solvents were dried, distilled and degassed before use. Elemental analyses were by the Canadian Microanalytical Service, Delta, BC. Preparative TLC was carried out on glass plates (20 × 20 cm) coated with silica (Merck 60 GF254, 0.5 mm thick).

4.1.1. Instrumentation

IR: Perkin–Elmer FT-IR 1920X. Solution spectra were obtained using a solution cell fitted with NaCl windows (path length 0.5 mm). Nujol mull spectra were collected from samples mounted between NaCl discs. NMR: samples were dissolved in $CDCl_3$ (Aldrich) using 5 mm sample tubes. Spectra were recorded using a Varian Gemini 200 instrument (^1H at 199.98 MHz, ^{13}C at 50.29 MHz). Electrospray (ES) mass spectra were obtained by direct diffusion of solutions in MeOH (unless otherwise indicated) into a Finnegan LCQ instrument. Nitrogen was used as the drying and nebulising gas. Chemical aids to ionisation are indicated where used [12].

4.1.2. Reagents

The compounds $W(C{\equiv}CC{\equiv}CH)(CO)_3Cp$ [10], $IrCl(CO)(PPh_3)_2$ [32] and $RhCl(CO)(PPh_3)_2$ [33] were prepared by the cited methods.

4.2. Preparation of $\{Cp(OC)_3W\}C{\equiv}CC{\equiv}C\{M(CO)(PPh_3)_2\}$ (M = Ir, Rh)

4.2.1. M = Ir (1)

A solution of $IrCl(CO)(PPh_3)_2$ (200 mg, 0.25 mmol) and AgOTf (66 mg, 0.25 mmol) in CH_2Cl_2 (20 ml) was stirred at room temperature (r.t.) for 3 h. The yellow solution was filtered under nitrogen into a Schlenk tube

and concentrated to 5 ml. $NHEt_2$ (30 ml) was added, followed by $W(C{\equiv}CC{\equiv}CH)(CO)_3Cp$ (98 mg, 0.25 mmol) and the solution was stirred for 1 h. The bright yellow precipitate of $\{Cp(OC)_3W\}C{\equiv}CC{\equiv}C\{Ir(CO)(PPh_3)_2\}$ (**1**) (230 mg, 80%) was collected by vacuum filtration and washed with hexane, with strict exclusion of air. Anal. Found: C, 52.29; H, 3.45. Calc. for $C_{49}H_{35}IrO_4P_2W$: C, 52.28; H, 3.13%; M, 1126. IR (CH_2Cl_2): ν(CO): 2037, 1952 cm^{-1}. ^{1}H-NMR: δ 5.55 (s, 5H, Cp), 7.39–7.75 (m, 30H, Ph). ^{13}C-NMR: δ 91.59 (s, Cp), 128.13–134.92 (m, Ph), 211.89 (s, W–CO), 231.62 (s, W–CO), 240.25 (s, Ir–CO). ES mass spectra (MeOH, m/z): 1126, M^+; 1098, $[M-CO]^+$; 745, $[Ir(CO)(PPh_3)_2]^+$.

4.2.2. $M = Rh$ (**2**)

This complex was prepared in a similar manner to **1**, using $RhCl(CO)(PPh_3)_2$ (200 mg, 0.28 mmol), AgOTf (74 mg, 0.28 mmol) and $W(C{\equiv}CC{\equiv}CH)(CO)_3Cp$ (110 mg, 0.28 mmol) in CH_2Cl_2 (20 ml) and $NHEt_2$ (30 ml). The yellow precipitate of $\{Cp(OC)_3W\}C{\equiv}CC{\equiv}C\{Rh(CO)(PPh_3)_2\}$ (**2**) (235 mg, 81%) was collected by vacuum filtration and washed with hexane, again with strict exclusion of air. Anal. Found: C, 56.95; H, 3.62. Calc. for $C_{49}H_{35}O_4P_2RhW$: C, 56.78; H, 3.40%; M, 1036. IR (CH_2Cl_2): ν(CO): 1952, 1973, 2037 cm^{-1}. ^{1}H-NMR: δ 5.47 (s, 5H, Cp), 7.40–7.75 (m, 30H, Ph). ^{13}C-NMR: δ 91.6 (s, Cp), 128.2–134.8 (m, Ph), 210.8 (s, W–CO), 231.6 (s, W–CO), 239.8 (s, Rh–CO). ES mass spectrum (with NaOMe, m/z): (positive ion mode) 1059, $[M+Na]^+$; (negative ion mode) 1067, $[M+OMe]^-$.

4.3. Reaction with iodomethane

4.3.1. $\{Cp(OC)_3W\}C{\equiv}CC{\equiv}C[IrMeI(CO)(PPh_3)_2]$ (**3**)

Iodomethane (0.25 ml, 0.4 mmol) was added to a solution of **1** (100 mg, 0.08 mmol) in thf (20 ml), and the resulting solution was stirred in the dark for 1 h. The solvent and any unreacted iodomethane were removed under vacuum and the residue was purified by preparative TLC (4:6 acetone–hexane, R_f 0.47) to give $\{Cp(OC)_3W\}C{\equiv}CC{\equiv}C\{IrMeI(CO)(PPh_3)_2\}$ (**3**) (85 mg, 76%). Anal. Found: C, 47.95; H, 3.3 1. Calc. for $C_{50}H_{38}IrO_4P_2W$: C, 47.37; H, 3.02%; M, 1268. IR (CH_2Cl_2): ν(CO) 2047, 2037, 1950 cm^{-1}. ^{1}H-NMR: δ 0.68 [t, $^3J(HP) = 5.4$ Hz, 3H, Me], 5.54 (s, 5H, Cp), 7.32–8.03 (m, 30H, Ph). ^{13}C-NMR: δ 1.11 (s, Me), 91.64 (s, Cp), 127.63–131.72 (m, Ph), 169.15 (s, Ir–CO), 210.80 (s, W–CO), 230.76 (s, W–CO). ES mass spectrum (MeOH, with NaOMe, m/z): 1291, $[M+Na]^+$; 1143, $[M-I]^+$.

4.4. Reactions with tetracyanoethene

4.4.1. $\{Cp(OC)_3W\}C{\equiv}CC{\equiv}C\{Ir(CO)[\eta\text{-}C_2(CN)_4](PPh_3)_2\}$ (**4**)

To a solution of **1** (104 mg, 0.09 mmol) in thf (15 ml), tcne (12 mg, 0.09 mmol) was added. The solution was stirred in the dark at 4°C for 20 min. Purification by preparative TLC (4:6 acetone–hexane, R_f 0.43) $\{Cp(OC)_3W\}C{\equiv}CC{\equiv}C\{Ir(CO)[\eta\text{-}C_2(CN)_4](PPh_3)_2\}$ (**4**) (87 mg, 78%). Anal. Found: C, 52.63; H 2.98; N, 4.50. Calc. for $C_{55}H_{35}N_4IrO_4P_2W$: C, 52.68; H, 2.8 1; N, 4.46%; M, 1254. IR (CH_2Cl_2): ν(CN) 2227, ν(CO) 2058, 2039, 1952 cm^{-1}. ^{1}H-NMR: δ 5.53 (s, 511, Cp), 7.26–7.52 (m, 30H, Ph). ^{13}C-NMR: δ 91.83 (s, Cp), 112.66, 116.95 (CN), 128.32–134.26 (m, Ph), 170.00 (s, Ir–CO), 211.17 (s, W–CO), 230.63 (s, W–CO). ES mass spectrum (MeOH, with NaOMe, m/z): 1277, $[M+Na]^+$; 1149, $[(M+Na)-C_2(CN)_4]^+$.

4.4.2. $\{Cp(OC)_3W\}C{\equiv}CC{\equiv}C\{Rh(CO)[\eta\text{-}C_2(CN)_4](PPh_3)_2\}$ (**5**)

The colour of a solution of **2** (100 mg, 0.09 mmol) in thf (20 ml) changed rapidly from yellow to orange when tcne (12.3 mg, 0.09 mmol) was added. After stirring in the dark at r.t. for 1 h, solvent was removed under vacuum and the residue purified by preparative TLC (4:3 acetone–hexane, R_f 0.35) which afforded $\{Cp(OC)_3W\}C{\equiv}CC{\equiv}C\{Rh(CO)[\eta\text{-}C_2(CN)_4](PPh_3)_2\}$ (**5**) as an orange crystalline solid (80 mg, 72%). Anal. Found: C, 53.67; H, 3.02; N, 4.44. Calc. for $C_{55}H_{35}N_4O_4P_2RhW{\cdot}CH_2Cl_2$: C, 53.82; H, 2.98; N, 4.48%; M, 1164. IR (CH_2Cl_2): ν(CN), 2224; ν(CC), 2142; ν(CO): 2078, 2039, 1953 cm^{-1}. ^{1}H-NMR: δ 5.51 (s, 5H, Cp), 7.29–7.57 (m, 30H, Ph). ^{13}C-NMR: δ 91.64 (s, Cp), 112.71, 116.72 (CN), 128.26–134.15 (m, Ph), 211.11 (s, W–CO), 230.79 (s, W–CO). ES mass spectrum (MeOH, m/z): 1036, $[M-C_2(CN)_4]^+$.

4.5. Reactions with $Fe_2(CO)_9$

4.5.1. $\{Cp(OC)_3W\}C{\equiv}CC_2\{Fe_2Ir(CO)_8(PPh_3)\}$ (**6**)

A suspension of **1** (100 mg, 0.089 mmol) and $Fe_2(CO)_9$ (143 mg, 0.39 mmol) in thf (30 ml) was heated at reflux point for 1 h. The solvent was removed under vacuum and isolation of the product by preparative TLC (4:6 CH_2Cl_2–hexane) gave a dark red band (R_f 0.43) that was recrystallised from CH_2Cl_2–hexane to give $\{Cp(OC)_3W\}C{\equiv}C_2\{Fe_2Ir(CO)_8(PPh_3)\}$ (**6**) as a red crystalline solid (7 mg, 7%) which analysed consistently for a $2CH_2Cl_2$-solvate. Anal. Found: C, 35.91, 35.73; H, 1.52, 1.57. Calc. for $C_{38}H_{20}Fe_2IrO_{11}PW{\cdot}2CH_2Cl_2$: C, 35.82; H, 1.80%; M, 1171. IR (cyclohexane): ν(CO) 2068, 2054, 2029, 2021, 2014, 2003, 1986, 1965, 1951 cm^{-1}. ^{1}H-NMR: δ 5.60 (s, 5H, Cp), 7.26–7.52 (m, 15H, Ph). ^{13}C-NMR: δ 88.39 (s, Cp), 128.79–133.88 (m, Ph), 212.07 (s, Fe–CO), 218.46 (s, W–CO). ES mass spectrum (MeOH, with NaOMe, m/z): 1202, $[M+OMe]^-$; 1174–1062, $[(M+OMe)-nCO]^-$ ($n = 1$–5); 940–854, $[(M+OMe)-nCO-PPh_3]^-$ ($n = 0$–3).

*4.5.2. {Cp(OC)$_3$W}C≡CC$_2${Fe$_2$Rh(CO)$_8$(PPh$_3$)} (**7**)*

A suspension of 2 (100 mg, 0.09 mmol) and $Fe_2(CO)_9$ (174 mg, 0.48 mmol) in thf (20 ml) was heated at reflux point for 2 h. The solvent was removed under vacuum and the residue purified by preparative TLC (4:6 CH_2Cl_2–hexane, R_f 0.39) to give dark red crystals of {Cp(OC)$_3$W}C≡CC$_2${Fe$_2$Rh(CO)$_8$(PPh$_3$)} (**7**) (35 mg, 37%). IR (cyclohexane): ν(CO) 2065, 2041, 2014, 1978, 1963, 1952 cm^{-1}. ^{1}H-NMR: δ 5.49 (s, 5H, Cp), 7.30–7.43 (m, 30H, Ph). ^{13}C-NMR: δ 91.72 (s, Cp), 128.35–134.22 (m, Ph), 167.70 (s, Rh–CO), 210.33 (s, W–CO), 212.52 (s, FeCO). ES mass spectrum (MeOH, with NaOMe, m/z): 1084, $[M + OMe]^-$.

*4.5.3. {Cp(OC)$_8$Fe$_2$W}C$_2$C$_2${Fe$_2$Ir(CO)$_8$(PPh$_3$)} (**8**)*

A suspension of **1** (100 mg, 0.089 mmol) and $Fe_2(CO)_9$ (143 mg, 0.39 mmol) in thf (30 ml) was heated at reflux point for 1 h. The solvent was removed under vacuum and isolation of the product by preparative TLC (4/6 CH_2Cl_2–hexane) gave a dark red band (R_f 0.48) that was recrystallised from CH_2Cl_2–hexane to give {Cp(OC)$_8$Fe$_2$W}C$_2$C$_2${Fe$_2$Ir(CO)$_8$(PPh$_3$)} (**8**) as a red crystalline solid (28 mg, 22%). Anal. Found: C, 35.89; H, 1.49. Calc. for $C_{43}H_{20}Fe_4IrO_{16}PW$: C, 36.29; H, 1.41%; M, 1423. IR (cyclohexane): ν(CO) 2063, 2041, 2026, 2013, 1999, 1962, 1951 cm^{-1}. ^{1}H-NMR: δ 5.63 (s, 511, Cp), 7.34–7.50 (m, 1511, Ph). ^{13}C-NMR: δ 91.94 (s, Cp), 128.57–133.74 (m, Ph), 174.80 (s, Ir–CO), 210.54 (s, Fe–CO), 212.39 (s, Fe–CO), 227.94 (s, W–CO). ES mass spectrum (MeOH, with NaOMe, m/z): 1454, $[M + OMe]^-$; 1342, $[(M + OMe) - 4CO]^-$; 1228, $[(M + OMe) - 8CO]^-$; 1147, $[(M + OMe) - 11CO]^-$.

*4.5.4. {Cp(OC)$_8$Fe$_2$W}C$_2$C$_2${Fe$_2$Rh(CO)$_8$(PPh$_3$)} (**9**)*

A suspension of **2** (100 mg, 0.09 mmol) and $Fe_2(CO)_9$ (174 mg, 0.48 mmol) in thf (20 ml) was heated at reflux point for 2 h. The solvent was removed under vacuum and the residue purified by preparative TLC (4/6 CH_2Cl_2–hexane, R_f 0.39) to give a red solid that was recrystallised with CH_2Cl_2–hexane to give crystals of **6**. The mother liquor was further purified by preparative TLC and crystallisation (CH_2Cl_2–hexane) to give {Cp(OC)$_8$Fe$_2$W}C$_2$C$_2${Fe$_2$Rh(CO)$_8$(PPh$_3$)} (**9**) (5 mg, 6%). Anal. Found: C, 38.15; H, 1.51. Calc. for $C_{43}H_{20}Fe_4O_{16}PRhW$: C, 38.72; H, 1.5 1%; M, 1334. IR (CH_2Cl_2): ν(CO) 2089, 2066, 2039, 2012, 1974, 1959, 1833 cm^{-1}. ES mass spectrum (MeOH, m/z): 1335, $[M + H]^+$; 1307, $[M - CO]^+$; 1113 $[M - Fe_2(CO)_4]^+$; 1073, $[M - PPh_3]^+$; 1046, $[M - CO - PPh_3]^+$.

5. Crystallography

Full spheres of data to $2\theta = 58°$ were measured at ca. 153 K using a Bruker AXS CCD area-detector instrument, merged to unique sets after 'empirical' absorption corrections (processing by proprietary software SMART, SAINT, SADABS, XPREP) [34]. N_{tot} data merged to N unique (R_{int}, quoted), N_o with $F > 4\sigma(F)$ being used in the refinements. All data were measured using monochromatic Mo–Kα radiation, $\lambda = 0.71073$ Å. In the refinements, anisotropic thermal parameter forms were used for the non-hydrogen atoms, (x, y, z, U_{iso}) being constrained at estimated values. Conventional residuals R, R_w on $|F|$ are quoted, statistical weights being employed. Neutral atom complex scattering factors were used; computation used the XTAL 3.4 program system [35]. Pertinent results are given in the figures (which show non-hydrogen atoms with 50% probability amplitude displacement ellipsoids) and tables.

5.1. Crystal and refinement data

*5.1.1. {Cp(OC)$_3$W}C≡CC≡C{Rh(CO)[η-C$_2$(CN)$_4$]-(PPh$_3$)$_2$}·3CH$_2$Cl$_2$ (**5**)*

$C_{55}H_{35}N_4O_4P_2RhW{\cdot}3CH_2Cl_2$: space group $P\bar{1}$, $a = 12.107(3)$, $b = 15.774(4)$, $c = 15.911(4)$ Å, ($\alpha = 80.696(5)$, $\beta = 81.864(5)$, $\gamma = 85.910(5)°$, $V = 2965$ Å^3, $Z = 2$. $D_{calc} = 1.590$ g cm^{-3}; $F(000) = 1400$. $\mu_{Mo} = 26$ cm^{-1}; specimen: $0.28 \times 0.14 \times 0.05$ mm; $T_{min,max} = 0.69$, 0.84. $N_{tot} = 22\,496$, $N = 10\,384$ ($R_{int} = 0.043$), $N_o = 4820$, $R = 0.064$, $R_w = 0.057$. $n_v = 678$; $|\Delta\rho| = 1.3(2)$ e Å^{-3}.

Variata. Phenyl ring C(22n) was modelled as disordered over two sets of sites, occupancy set at 0.5 for each after trial refinement. A nearby void contained residues modelled as dichloromethane (3) disordered over two sets of sites with similar occupancy, possibly concerted with the disorder of the phenyl ring.

*5.1.2. {Cp(OC)$_3$W}C≡CC$_2${Fe$_2$Rh(CO)$_8$(PPh$_3$)} (**7**)*

$C_{38}H_{20}Fe_2O_{11}PRhW$: triclinic, space group $P\bar{1}$, $a = 12.490(2)$, $b = 12.485(2)$, $c = 13.439(2)$ Å, $\alpha = 62.909(1)$, $\beta = 72.647(1)$, $\gamma = 75.881(1)°$, $V = 1817$ Å^3, $Z = 2$. $D_{calc} = 1.977$ g cm^{-3}; $F(000) = 1044$. $\mu_{Mo} = 45$ cm^{-1}; specimen: $0.40 \times 0.22 \times 0.$ 12 mm; $T_{min,max} = 0.64$, 0.93. $N_{tot} = 20\,883$, $N = 8923$ ($R_{int} = 0.022$), $N_o = 7930$, $R = 0.021$, $R_w = 0.026$. $n_v = 487$; $|\Delta\rho| = 1.4(1)$ e Å^{-3}.

*5.1.3. {Cp(OC)$_8$Fe$_2$W}C$_2$C$_2${Fe$_2$Ir(CO)$_8$(PPh$_3$)} (**8**)*

$C_{43}H_{20}Fe_4IrO_{16}PW$: triclinic, space group $P\bar{1}$, $a = 10.269(1)$, $b = 14.025(2)$, $c = 16.889(2)$ Å, $\alpha = 109.808(2)$, $\beta = 96.566(2)$, $\gamma = 100.671(2)°$, $V = 2207$ Å^3, $Z = 2$. $D_{calc} = 2.141$ g cm^{-3}; $F(000) = 1352$. $\mu_{Mo} = 70$ cm^{-1}; specimen: $0.20 \times 0.10 \times 0.06$ mm; $T_{min,max} = 0.67$, 0.95. $N_{tot} = 25\,318$, $N = 10\,635$ ($R_{int} = 0.026$), $N_o = 8407$, $R = 0.030$, $R_w = 0.050$. $n_v = 596$; $|\Delta\rho| = 2.8(1)$ e A^{-3}.

6. Supplementary material

Crystallographic data for the structure determinations have been deposited with the Cambridge Crystallographic Data Centre as CCDC 140684–6 for compounds **5**, **7** and **8**, respectively. Copies of this information may be obtained free of charge from: The Director, CCDC, 12 Union Road, Cambridge, CB2 1EZ, UK (Fax: +44-1223-336-033; e-mail: deposit@ccdc.cam.ac.uk or www: http://www.ccdc.cam.ac.uk).

Acknowledgements

We thank the Australian Research Council for support of this work and J.F. Krieg for some preliminary experiments.

References

[1] (a) U.H.F. Burtz, Angew. Chem. Int. Ed. Engl. 35 (1996) 969. (b) H. Lang, Angew. Chem. Int. Ed. Engl. 33 (1994) 547. (c) W. Beck, B. Neimer, H. Wieser, Angew. Chem. Int. Ed. Engl. 32 (1993) 923. (d) H. Iwamura, K. Matsuda, in: P.J. Stang, F. Diederich (Eds.), Modern Acetylenic Chemistry, VCH, Weinheim, 1995. (e) F. Paul, C. Lapinte, Coord. Chem. Rev. 178–180 (1998) 431.

[2] (a) I.R. Whittall, A.M. McDonagh, M.G. Humphrey, M. Samoc, Adv. Organomet. Chem. 42 (1998) 291. (b) S. Houbrechts, C. Boutton, K. Clays, A. Persoons, I.R. Whittall, R.H. Naulty, M.P. Cifuentes, M.G. Humphrey, J. Nonlinear Opt. Phys. Mat. 7 (1998) 113. (c) R.H. Naulty, A.M. McDonagh, I.R. Whittall, M.P. Cifuentes, M.G. Humphrey, S. Houbrechts, J. Maes, A. Persoons, G.A. Heath, D.C.R. Hockless, J. Organomet. Chem. 563 (1998) 137. (d) I.Y. Lu, J.T. Lin, J. Luo, C.-S. Li, C. Tsai, Y.S. Wen, C.-C. Hsu, F.-F. Yeh, S. Liou, Organometallics 17 (1998) 2188. (e) N.J. Long, Angew. Chem. Int. Ed. Engl. 34 (1995) 21 and references therein.

[3] F. Paul, C. Lapinte, Coord. Chem. Rev. 178–180 (1998) 431.

[4] (a) M. Brady, W. Weng, Y. Zhou, J.W. Seyler, A.J. Amoroso, A.M. Arif, M. Bohme, G. Frenking, J.A. Gladysz, J. Am. Chem. Soc. 119 (1997) 775. (b) F. Coat, M.-X Guillevic, L. Toupet, F. Paul, C. Lapinte, Organometallics 16 (1997) 5988. (c) M.I. Bruce, P.J. Low, K. Costuas, J.-F. Halet, S.P. Best, G.A. Heath, J. Am. Chem. Soc. 122 (2000) 1949. (d) S. Kheradmandan, K. Heinze, H.W. Schmalle, H. Berke, Angew. Chem. Int. Ed. Engl. 38 (1999) 2270.

[5] (a) V.M. Mel'nichenko, A.M. Sladkov, Yu.N. Nikulin, Russ. Chem. Rev. 51 (1982) 421. (b) P.P.K. Smith, P.R. Busek, Science 216 (1982) 984. (c) Yu.P. Kudryatsev, S. Evsyukov, M. Guseva, V. Babaev, V. Khvostov, in: P.A. Thrower (Ed.), Chemistry and Physics of Carbon, vol. 25, Marcel Dekker, New York, 1997, p. 1.

[6] M.I. Bruce, B.C. Hall, P.J. Low, M.E. Smith, B.W. Skelton, A.H. White, Inorg. Chim. Acta 300–302 (2000) 633.

[7] W. Weng, T. Bartik, M. Brady, B. Bartik, J.A. Ramsden, A.M. Arif, J.A. Gladysz, J. Am. Chem. Soc. 117 (1995) 11922.

[8] (a) D. Strope, D.F. Shriver, Inorg. Chem. 13 (1974) 2652. (b) C. Eaborn, N. Farrell, J.L. Murphy, A. Pidcock, J. Chem. Soc. Dalton Trans. (1976) 58.

[9] M.I. Bruce, M. Ke, P.J. Low, B.W. Skelton, A.H. White, Organometallics 17 (1998) 3539.

[10] W. Beck, H. Bauer, B. Olgemöller, Inorg. Synth. 26 (1989) 120.

[11] R.H. Walter, B.F.G. Johnson, J. Chem. Soc. Dalton Trans. (1978) 381.

[12] (a) B.K. Nicholson, W. Henderson, J. Chem. Soc. Chem. Commun. (1995) 2531. (b) W. Henderson, J.S. McIndoe, B.K. Nicholson, P.J. Dyson, J. Chem. Soc. Chem. Commun. (1996) 1183.

[13] M.I. Bruce, A.G. Swincer, Adv. Organomet. Chem. 22 (1983) 59.

[14] R.F. Heck, J. Org. Chem. 28 (1963) 604.

[15] M.I. Bruce, R.C. Wallis, Aust. J. Chem. 32 (1979) 1471.

[16] (a) W.H. Baddley, J. Am. Chem. Soc. 88 (1966) 4545. (b) J.P. Collman, J.W. Kang, J. Am. Chem. Soc. 89 (1967) 844.

[17] M.I. Bruce, T.W. Hambley, M.R. Snow, A.G. Swincer, Organometallics 4 (1985) 501.

[18] (a) C.K. Brown, D. Georgiou, G. Wilkinson, J. Chem. Soc. Dalton Trans. (1971) 3120. (b) M.I. Bruce, T.W. Hambley, M.R. Snow, A.G. Swincer, J. Organomet. Chem. 235 (1982) 105.

[19] C.S. Chin, M. Oh, G. Won, H. Cho, D. Shin, Polyhedron 18 (1999) 811.

[20] J.B.R. Dunn, R. Jacobs, C.J. Frithie Jr, J. Chem. Soc. Dalton Trans. (1972) 2007.

[21] P. Becker, P. Coppens, F.K. Ross, J. Am. Chem. Soc. 95 (1973) 7604.

[22] J.A. McGinnety, J.A. Ibers, J. Chem. Soc. Chem. Commun. (1968) 235.

[23] M.I. Bruce, P.J. Low, B.W. Skelton, A.H. White, unpublished results.

[24] N.A. Ustynyuk, V.N. Vinogradova, V.N. Korneva, Yu.L. Slovokhotov, Yu.T. Struchkov, Koord. Khim. 9 (1983) 631.

[25] L. Busetto, J.C. Jeffery, R.M. Mills, F.G.A. Stone, M.J. Went, P. Woodward, J. Chem. Soc. Dalton Trans. (1983) 101.

[26] M.I. Bruce, G. Koutsantonis, E.R.T. Tiekink, J. Organomet. Chem. 407 (1991) 391.

[27] (a) S. Deabate, R. Giordano, E. Sappa, J. Cluster Sci. 8 (1997) 407. (b) P.R. Raithby, M.J. Rosales, Adv. Inorg. Chem. Radiochem. 29 (1985) 169. (c) E. Sappa, A. Tiripicchio, P. Braunstein, Chem. Rev. 83 (1983) 203.

[28] K. Yasufuku, K. Aoki, H. Yamazaki, Bull. Chem. Soc. Jpn. 48 (1975) 1616.

[29] J.C. Jeffery, K.A. Mead, H. Razay, F.G.A. Stone, M.J. Went, P. Woodward, J. Chem. Soc. Dalton Trans. (1984) 1383.

[30] L.J. Farrugia, J. Organomet. Chem. 310 (1986) 67.

[31] D.M. Norton, C.L. Stern, D.F. Shriver, Inorg. Chem. 33 (1994) 2701.

[32] J.P. Collman, C.T. Sears Jr., M. Kubota, Inorg. Synth. 28 (1990) 92.

[33] D. Evans, J.A. Osborn, G. Wilkinson, Inorg. Synth. 28 (1990) 79.

[34] (a) G. Sheldrick, SADABS, Siemens Area Detector Absorption Correction Program, 1996. (b) SMART, Area Detector Software Package and SAINT, Sax Area Detector Integration Program, Siemens Industrial Automation, Inc., Madison, 1995.

[35] S.R. Hall, G.S.D. King, J.M. Stewart (Eds.), The XTAL 3.4 Users' Manual, University of Western Australia, Lamb, Perth, 1994.